OPTIMIZING NOISE BARRIERS WITH COMSOL MULTIPHYSICS

Patrick Grahn[1], **Mads Herring Jensen** [2]

[1] COMSOL Oy
Arabiankatu 12
00560 Helsinki
patrick@comsol.fi

[2] COMSOL A/S
Diplomvej 381
2800 Kgs. Lyngby
mads@comsol.dk

Abstract

Road noise is a major concern in urban environments. A common countermeasure is installation of roadside noise barriers. However, the effectiveness of barriers is limited by a number of restrictive factors such as cost, maximum height, materials and surrounding infrastructure. Thus, there is a need to design the optimal wall structure for different situations. In this article, we model the sound attenuation by four different noise barrier designs and compare their performance with in situ measurements. We find that numerical simulations enable efficient optimization of barrier designs and, thereby, greatly reduces the need for physical prototypes.

1 INTRODUCTION

The increasing concern about noise pollution has pushed the development of new methods that mitigate traffic-borne noise in residential areas. One of the most efficient methods is the use of noise barriers. In fact, there exists a wide variety of designs to choose from, ranging from absorbing and dispersive barriers to vegetation and barriers with novel tops [1]. In order to optimize the noise reduction per invested money, it is important to understand how different barrier designs perform in the desired environment. For this purpose, numerical modeling is an invaluable tool when deciding upon the best barrier design.

In this paper, we start by presenting the diffraction theory that describes the basic operation of noise barriers. Then, we introduce noise tops that can be placed on top of the barriers in order to further improve noise reduction. Finally, a numerical model built with COMSOL Multiphysics is used to investigate the performance of four different top designs: L-top, Watts-top and two sizes of T-tops. The model's results are compared to experimental data published by the Danish Road Directorate [2].

2 MODELING NOISE BARRIERS

In its simplest form, a noise barrier is a vertical wall that reflects or absorbs acoustic waves. At first, one could think that if a large vertical wall blocks the view to noise sources, then complete silence exists behind the wall. Unfortunately, this is not the case. Noise consists of acoustic pressure waves that have a finite wavelength. These waves experience diffraction at the edges of an obstruction and, thereby, secondary pressure waves are scattered into the geometrical shadow of the wall. Consequently, noise is observed behind an impenetrable noise barrier. In order to quantify this noise, we will take a brief look at the theory of scalar wave diffraction.

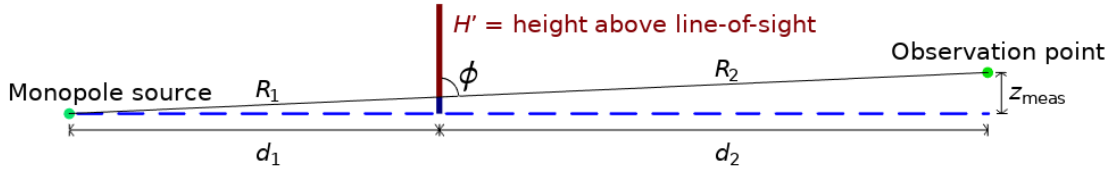

Figure 1. Diffraction by a thin vertical wall. The black line that connects source and observation point is the line-of-sight. The wall cuts the line-of-sight into two segments of lengths R_1 and R_2. The part of the barrier that is above the line-of-sight has a length H'.The source radiates into the upper half-space: the blue dashed line depicts ground.

The noise levels behind a thin vertical wall can be described by the Fresnel-Kirchhoff formulation of knife-edge diffraction [3]. Consider the setup shown in Figure 1. A monopole source is positioned at the origin, radiating a spherical wave of the following form

$$p_{\text{source}}(r) = p_0 \frac{r_{\text{ref}}}{r} e^{-\mathrm{j}kr}, \tag{1}$$

where $k = 2\pi/\lambda$ is the wave number and p_0 is the pressure magnitude at a reference distance r_{ref}. In the absence of ground reflections, the field behind the wall is obtained by the knife-edge diffraction solution

$$p_{\text{diff}}(\mathbf{r}) = \left(\frac{1+\mathrm{j}}{2}\right) p_0 \frac{r_{\text{ref}}}{R_1 + R_2} e^{-\mathrm{j}k(R_1+R_2)} \sqrt{\frac{2}{\pi}} \mathrm{F}\left(H' \sin\phi \sqrt{\frac{k}{2}\left(\frac{1}{R_1} + \frac{1}{R_2}\right)} \right), \tag{2}$$

where the geometrical lengths R_1, R_2 and H' are defined in Figure 1. The Fresnel integral $\mathrm{F}(\cdot)$ can be expressed in the following form

$$\mathrm{F}(u) = \left(\sqrt{\frac{\pi}{8}} - \int_0^u \cos(x^2)\, dx\right) - \mathrm{j}\left(\sqrt{\frac{\pi}{8}} - \int_0^u \sin(x^2)\, dx\right). \tag{3}$$

These integrals can be evaluated numerically.

If one assumes the ground to be a hard wall (infinite impedance), the ground reflections can be included by adding the solution in the mirror image of the observation point. For a coordinate system with z-axis normal to the ground plane, one obtains the equation

$$p_{\text{with ground}}(x, y, z) = p_{\text{diff}}(x, y, z) + p_{\text{diff}}(x, y, -z). \tag{4}$$

For both cases, with and without ground reflections, we define the insertion loss of the wall by comparing the sound pressure level behind the barrier to the sound pressure level in the absence of a barrier. In units of decibel, the insertion loss becomes

$$IL(\mathrm{dB}) = -20\log_{10}\left(\frac{|p(\mathbf{r})|}{|p_{\mathrm{source}}(r)|}\right), \tag{5}$$

where $p(\mathbf{r})$ can be evaluated from either Eq. (2) or Eq. (4). The insertion loss clearly depends on the location of measurement.

In the following, we consider a wall of 4 m total height, $d_1 = 13.5$ m, $d_2 = 20$ m and $z_{\mathrm{meas}} = 1.5$ m. Inserting these values into equations (1-5), allows us to plot the insertion loss in Figure 2. The figure shows that, in the absence of ground reflections, the insertion loss grows steadily with increasing frequency. At high frequencies the growth is fixed at 3 dB per octave. The same behavior generally holds when including the ground reflections, but now additional interference is added on top of the spectrum as can be seen by the green dashed line in Figure 2. The interference is caused by waves reaching the observation point by two distinct paths; directly from the wall or by reflection from the ground. Looking at the frequencies 280 Hz, 850 Hz, 1420 Hz, 1990 Hz and 2560 Hz, we have destructive interference and the insertion loss is exceptionally high. In contrast, at approximately 540 Hz, 1120 Hz, 1690 Hz and 2260 Hz, we have constructive interference, which reduces the insertion loss by about 5 dB compared to the blue curve. In principle, a maximum of 6 dB reduction is possible, if the two pressures in equation (4) are of equal amplitude and phase.

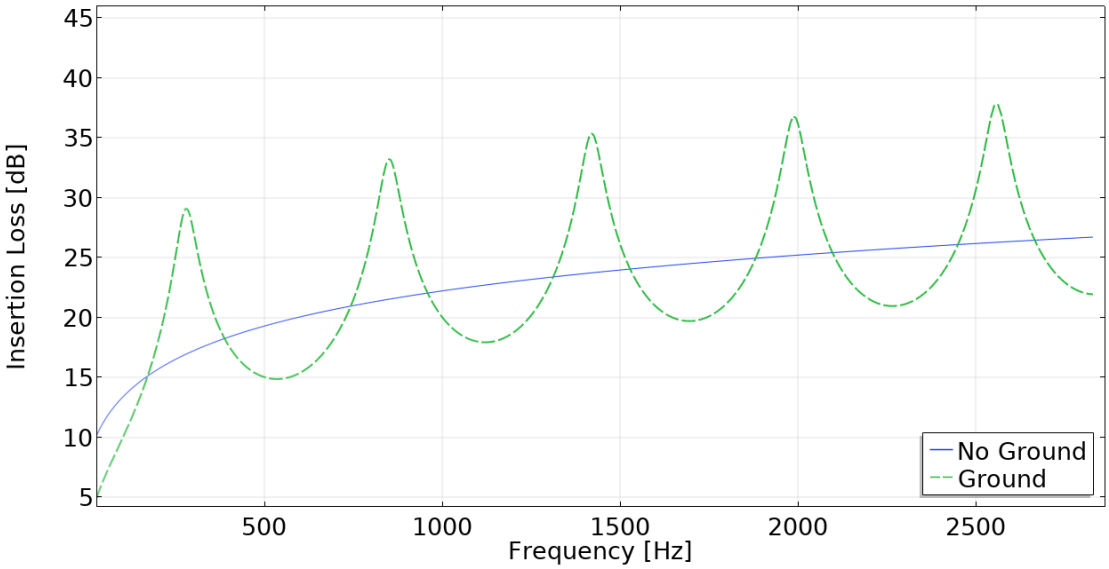

Figure 2. Insertion loss of a thin vertical wall calculated by equations (1-5). The blue solid line shows the case with no ground reflections. The green dashed line shows the case with reflecting hard ground.

Using the analytical equations, we can check that increasing the wall by 1 meter would increase insertion loss by approximately 2 dB. As growing the wall height to improve insertion loss may eventually get problematic, other options are sought after. One such option is to use barrier tops. These tops are placed at the top of the wall with the aim of suppressing the diffracted wave. Figure 3 depicts the noise tops considered in this work.

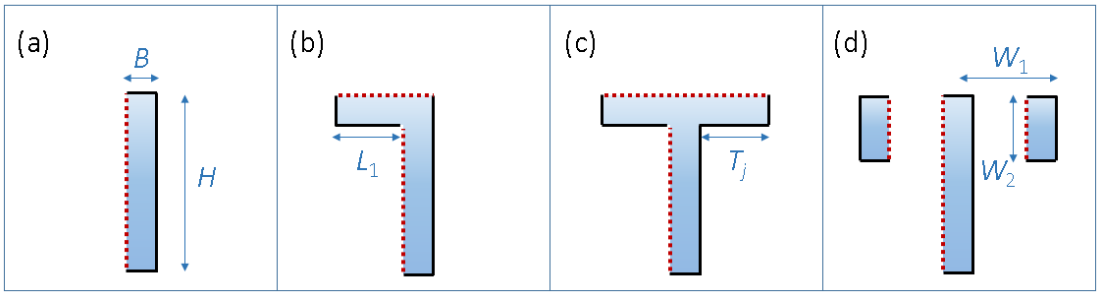

Figure 3. Cross sections of the noise barrier designs. The red dotted surfaces depict interfaces to sound-absorptive material (stone wool), whereas the black solid lines depict hard (metal) surfaces. The noise source is considered to be on the left side of the barrier. We consider the cases of (a) noise barrier without top, (b) L-top, (c) T-top of two variants and (d) Watts-top. The dimensions are $B = 0.16$ m, $H = 4$ m, $L_1 = 1$ m, $T_1 = 0.5$ m, $T_2 = 1$ m, $W_1 = 1$ m and $W_2 = 0.5$ m. We will refer to the two T-tops as the T1-top and T2-top based on whether T_1 or T_2 is used. All dimensions were chosen based on the project carried out by the Danish Road Directorate [2].

As the noise tops are of rather complicated shape, understanding their impact on the diffracted wave is rather difficult using only analytical equations. Instead, it is better to use finite-element models that accurately compute how the acoustic waves interact with the noise barrier. In contrast to analytical equations, the following effects can straightforwardly be included into a finite-element model: (I) interaction of pressure waves with noise tops of arbitrary geometrical shape, (II) absorbing materials in the noise barrier or top, (III) ground reflections using a realistic frequency-dependent impedance, (IV) use of different ground impedance models in different locations.

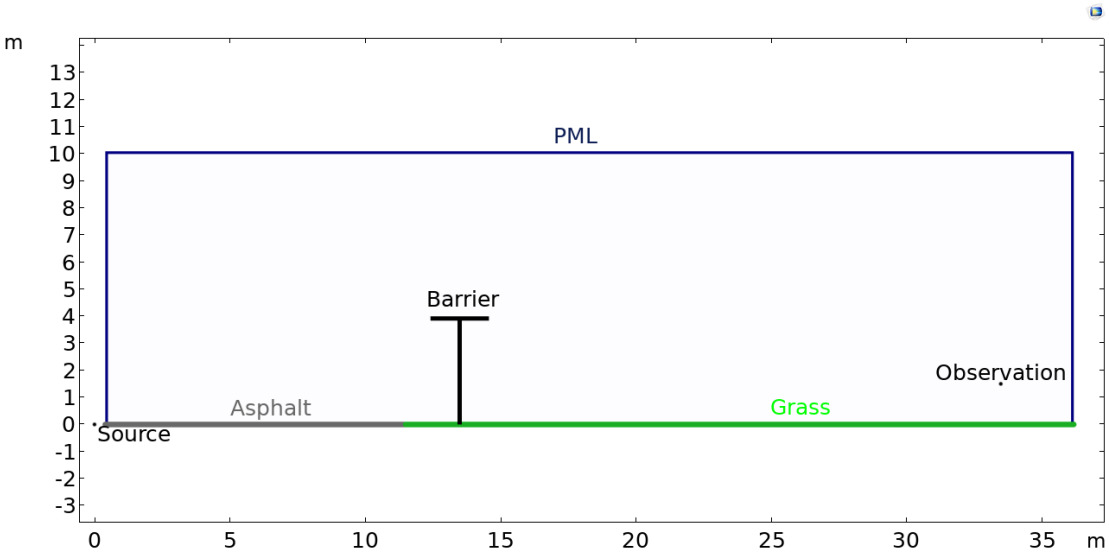

Figure 4. Geometry of the computational model. The figure shows a cross-section of the axisymmetric system in (ρ, z)-cylindrical coordinates. Impedance conditions are used to describe the asphalt, grass and sound-absorbing surfaces of the barrier. Perfectly matched layers (PML) are used to achieve impedance-matching to free-space for all waves escaping the modeling domain. The source lies outside the modeling domain. Therefore, its field is prescribed using a scattered-field formulation.

The setup of the finite-element model built with COMSOL Multiphysics is depicted in Figure 4. We employ a 2D-axisymmetric formulation in order to greatly reduce required

computational resources compared to a 3D model. The 2D-axisymmetric formulation allows us to define a noise source that creates spherical waves according to Eq. (1). A slight drawback is that the axisymmetric formulation makes the noise barrier curved. This approximation has a small influence on the absolute noise levels, but should not affect the conclusions presented in this work. It is also worth noting that noise barriers installed at real sites have finite lengths and may follow a curved road.

The sound absorbing surfaces are modeled with an impedance boundary condition. The frequency-dependent impedance is defined by the Attenborough model [4] that is a built-in feature in COMSOL. It is a semiempirical model with four parameters. They are the porosity ε_p, flow resistivity R_f, tortuosity factor τ_∞ and fitting parameter b. For the road, we consider 4 cm of asphalt with $\varepsilon_p = 0.2$, $R_f = 20000\ \mathrm{kPa \cdot s/m^2}$ and $\tau_\infty = 1.2$. The grass-covered ground is treated as a 20 cm layer of $\varepsilon_p = 0.7$, $R_f = 200\ \mathrm{kPa \cdot s/m^2}$ and $\tau_\infty = 1.2$. The barrier's absorptive surfaces were characterized by $\varepsilon_p = 0.8$, $R_f = 200\ \mathrm{kPa \cdot s/m^2}$ and $\tau_\infty = 1.5$, which are reported values from previous studies [5,6]. The fitting parameter $b = 1$ in all cases.

The model is solved up to the 2500 Hz third-octave band using 60 frequency samples in each third-octave band. We also consider the case without any barrier. The solution without a barrier is used to evaluate the insertion loss by equation (5), where in the place of p_{source} we use the computed pressure that is influenced by the asphalt and grass interfaces. For the solution process, the required computational resources grow with increasing frequency, because the acoustic field is described by a finite-element mesh that must resolve the wavelength. However, we were able to successfully solve the model using a single desktop computer with capacity to proceed even beyond 5000 Hz. The decision to stop at 2500 Hz was motivated by the experimental results.

3 RESULTS

The following results are obtained using a wall of 4 m total height, $d_1 = 13.5$ m, $d_2 = 20$ m and $z_{\mathrm{meas}} = 1.5$ m (see Figure 1)**.** The calculated sound pressure level (SPL) distribution depends on the frequency of the noise. As an example, the distribution at 1200 Hz is shown in Figure 5. The SPL at the observation point is seen to be significantly smaller than close to the source. The spreading of the spherical wave as it propagates to the observation point corresponds to about 30 dB reduction of SPL. The barrier adds additional reduction on the order of 20 dB. The reflection from the ground makes the SPL rather inhomogeneous, so the absolute SPL will strongly depend on the location of the observation point. However, the octave- or third-octave-averaged SPL is expected to be somewhat less sensitive on the exact location. In Figure 5(b), the T2-top has been added to the barrier. This brings additional 6 dB reduction of SPL at this particular frequency, which can be seen by the blue color being darker in the Figure 5(b) compared to Figure 5(a).

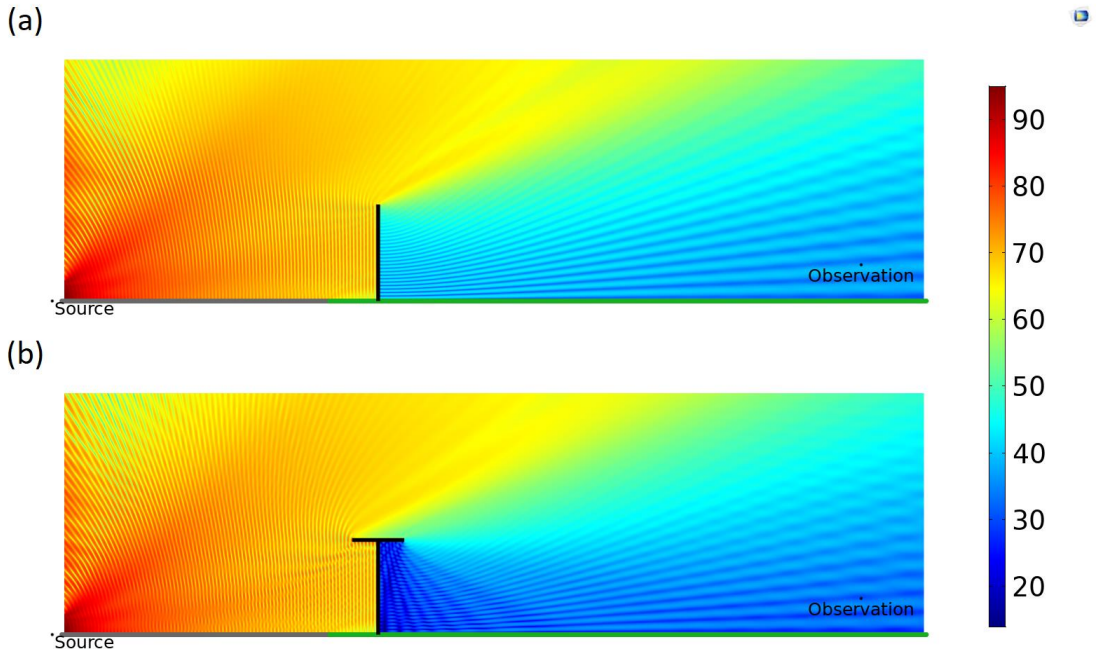

Figure 5. Computed sound pressure level in dB at 1200 Hz. The cases of (a) no top and (b) T2-top are shown. The ground is divided into asphalt (gray) and grass (green).

The insertion loss (IL) of the barrier design can be defined by Eq. (5). Figure 6 shows the computed IL as a function of frequency for five different cases. The considered cases are a barrier without a top and barriers with L-top, T1-top, T2-top and Watts-top.

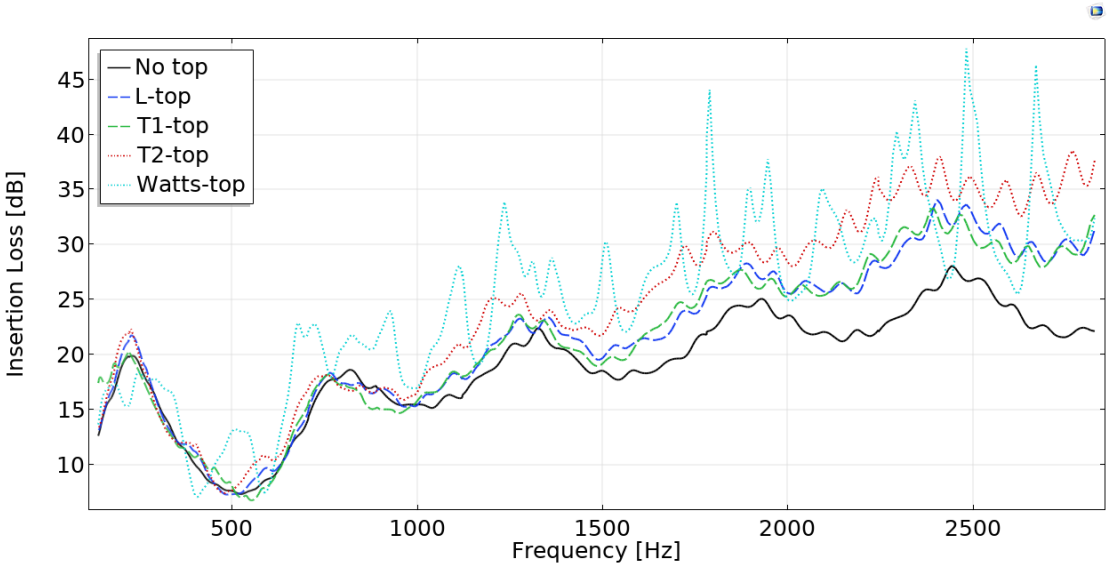

Figure 6. Computed insertion loss as a function of frequency. The black solid line is a 4-meter vertical wall with an absorptive surface towards the road. The colored dashed and dotted lines are for the same wall, but with the addition of one of the noise tops of Figure 3.

In the absence of a noise top, the computed insertion loss shares many features with the theoretical results of Figure 2. The constructive interference caused by ground reflections are clearly seen at the minima 540 Hz, 1120 Hz, 1690 Hz and 2260 Hz, but the effects are less pronounced due to the damping by the grassy terrain. Adding an L-top or T-top is seen to consistently increase insertion loss, especially at high frequencies. The wider T2-top is clearly more effective than its 1-meter counterpart. The results for the Watts top is interesting. Its three-part structure introduces additional interference effects that can greatly suppress the noise at selected frequencies. This interference can also reduce the insertion loss as observed within two narrow bands at 400 Hz and 570 Hz. However, this local reduction is small compared to the benefits obtained at frequencies around 1000 Hz, where A-weighted traffic noise is expected to be most prominent.

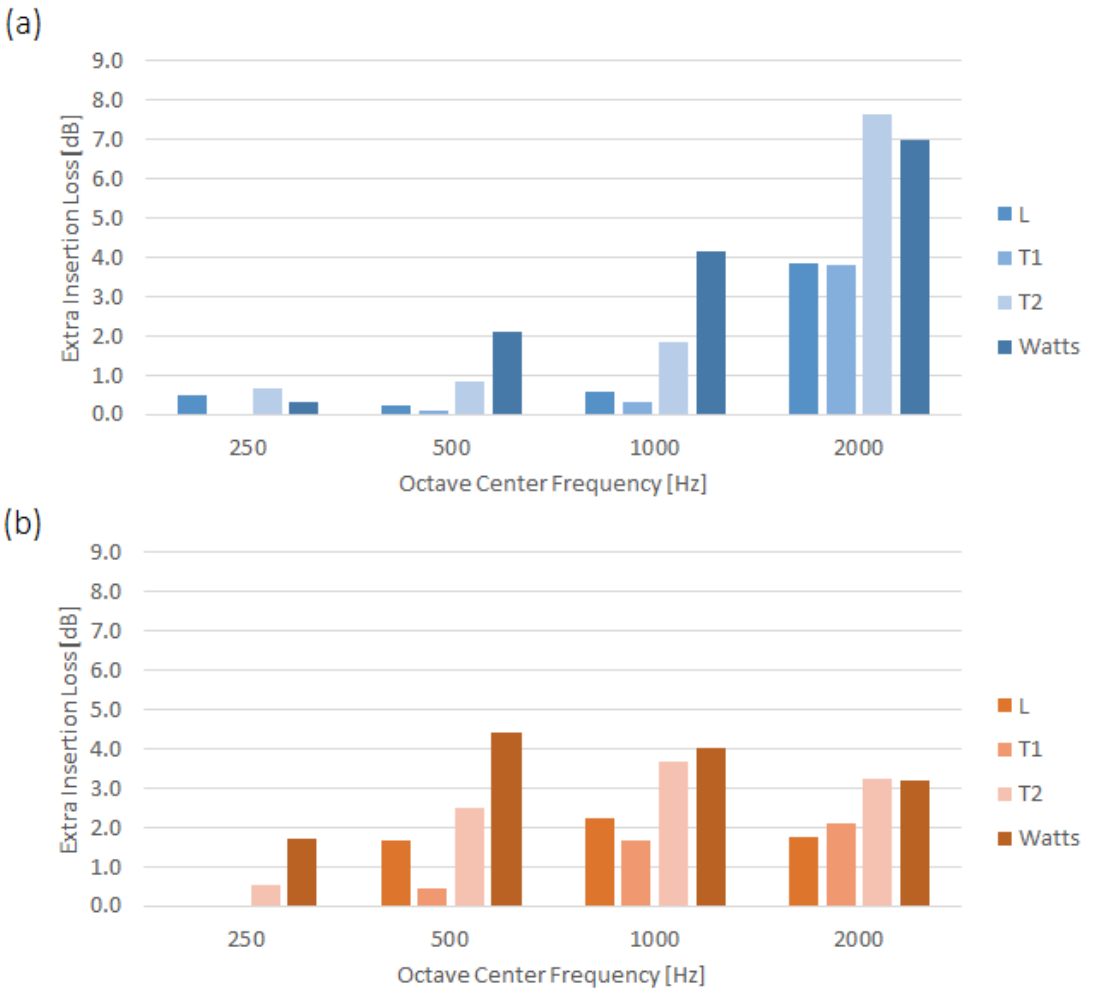

Figure 7. Extra insertion loss per octave obtained by adding a noise top to the barrier. Figure (a) shows the results obtained from the finite element model. Figure (b) shows the experimental results reported in Ref. [2]. The model defines the insertion loss as seen by an ideal omnidirectional microphone, whereas the experiments recorded the noise with a highly directional 2.4 m parabol system.

In order to get an overview of the noise tops' performance, we calculate the difference between the insertion loss of the barrier with a noise top and the loss of the barrier without a top. This difference is the extra insertion loss provided by the top. We are interested in comparing the extra insertion loss to the experimental values reported in Ref. [2]. In the experiment, the noise source was a wide motorway with four lanes. The two southbound lanes can be represented by a spherical wave source at a distance of $d_1 = 13.5$ m in front of the barrier, whereas the two northbound lanes would be at a distance of $d_1 = 25$ m. In order for the model to better represent the experimental setup, we perform two separate computations, one with $d_1 = 13.5$ m and one with $d_1 = 25$ m. Assuming the traffic noise to be nearly equal on the north- and southbound lanes, we can average the pressure magnitude of the two computations and use that to evaluate the insertion loss. The obtained motorway-insertion-loss is then collected into four octaves and plotted in Figure 7(a). For comparison, the experimental results for the same tops are shown in Figure 7(b).

There are some general trends that can be seen from both model and experiments. First, we see that the tops are ineffective in the 250 Hz band, but increase in effectiveness as the frequency increases. Second, we can see that the L-top and the T1-top are similar in performance. In the 500 Hz and 1000 Hz octaves, the Watts top is clearly the best choice, but at higher frequencies the T2-top is of similar or better performance. The choice between these two tops would be determined by the noise source spectrum. If noise suppression for a wide residential area is desired, it would also be necessary to average the extra insertion loss over many observation points. This could favor one top over another, as their diffraction patterns are rather different.

Looking at Figure 7, it is apparent that significant differences between model and experiment are seen in the 2000 Hz octave band. This difference is caused by the different ways of measuring noise. The parabol antenna used in the experimental setup had a very high directivity, especially at higher frequencies. At frequencies above 500 Hz, the parabol microphone was seen to suppress the ground effect interference patterns [2]. It was believed that the observed frequency dependence was a combination of the actual noise level in the sound field behind the barrier and the parabol amplification of the noise signal. In contrast, the finite element model did not include any amplification caused by a measurement system and hence it gives the noise level seen by an ideal omnidirectional microphone. This difference in measurement explains the observed discrepancy. These findings suggest that for a human listener, the performance of the noise tops at high frequencies is actually better than what was seen in the experiment. It should be emphasized that the influence of the ground effect on the overall noise will depend on the local terrain. Therefore, for most accurate results, we recommend to compute finite element models with source positions and terrains that match the final installation site of the barriers.

4 CONCLUSIONS

We have shown how the performance of noise barriers is determined by wave diffraction and reflection. Using COMSOL Multiphysics, we computed the performance of different noise tops situated on top of noise barriers. We saw that the noise tops can significantly improve the performance of a noise barrier, especially at frequencies beyond 1000 Hz. Our computed performance was compared to experimental data and some agreement was observed. Deviations between experiments and modeling were argued to originate from the directivity of the measurement microphone. The results suggest that noise tops have both frequency-dependent and directional noise suppression, which emphasizes that the best choice of noise top will always be situational. Using the presented computational model, we can rapidly create virtual prototypes in advance of a noise protection project. This will ensure that optimal noise suppression is achieved, prior to assembling the costly barrier on-site.

ACKNOWLEDGMENTS

We thank Gilles Pigasse, former member of Danish Road Directorate and COMSOL Multiphysics GmbH, for developing earlier versions of the simulation model and for sharing deep insight about the barrier elements and their material properties.

REFERENCES

[1] Pigasse G, Kragh J, "Optimised noise barriers – a state-of-the-art report", Vejdirektoratet (Danish Road Directorate), Report 194 (2011).

[2] Kragh J, Skov R S H, "Modified barrier tops – In-situ measurements of traffic noise attenuation by barriers with special tops", Vejdirektoratet (Danish Road Directorate), Report 539 (2015).

[3] Durgin G D, "The Practical Behavior of Various Edge-Diffraction Formulas", IEEE Antennas and Propagation Magazine 51 (2009), 24-35.

[4] Attenborough K, Bashir I, Taherzadeh S, "Outdoor ground impedance models", J. Acoust. Soc. Am. 129 (2011), 2806-2819.

[5] Pigasse G, "BEM calculations – Explanations of the Matlab code and the simulations", Vejdirektoratet (Danish Road Directorate), Internal Note (2010).

[6] Pigasse G, Kragh J, "Validation of the BEM program", Vejdirektoratet (Danish Road Directorate), Internal Note (2010).